# A high resolution record of Greenland mass balance

Malcolm McMillan[1*], Amber Leeson[2], Andrew Shepherd[1], Kate Briggs[1], Thomas W. K. Armitage[3], Anna Hogg[1], Peter Kuipers Munneke[4], Michiel van den Broeke[4], Brice Noël[4], Willem Jan van de Berg[4], Stefan Ligtenberg[4], Martin Horwath[5], Andreas Groh[5], Alan Muir[3] and Lin Gilbert[3].

1. Centre for Polar Observation and Modelling, University of Leeds, Leeds, LS2 9JT, UK.

2. Data Science Institute and Lancaster Environment Center, University of Lancaster, Lancaster, UK.

3. Centre for Polar Observation and Modelling, University College London, London, WC1E 6BT, UK.

4. Institute for Marine and Atmospheric Research, Utrecht University, Utrecht, The Netherlands.

5. Institut für Planetare Geoädsie, Technische Universität Dresden, 01062 Dresden, Germany.

*m.mcmillan@leeds.ac.uk

## Key points

1. Greenland contributed 0.74 ± 0.14 mm/yr to global mean sea level between 2011 and 2014.

2. Small scale mass deficits have made a relatively large contribution to recent ice loss.

3. High resolution radar altimetry can map Greenland mass balance at fine spatial and temporal resolution.

# Abstract

**We map recent Greenland Ice Sheet elevation change at high spatial (5-km) and temporal (monthly) resolution using CryoSat-2 altimetry. After correcting for the impact of changing snowpack properties associated with unprecedented surface melting in 2012, we find good agreement (3 cm/yr bias) with airborne measurements. With the aid of regional climate and firn modelling, we compute high spatial and temporal resolution records of Greenland mass evolution, which correlate (R=0.96) with monthly satellite gravimetry, and reveal glacier dynamic imbalance. During 2011-2014, Greenland mass loss averaged 269±51 Gt/yr. Atmospherically-driven losses were widespread, with surface melt variability driving large fluctuations in the annual mass deficit. Terminus regions of five dynamically-thinning glaciers, which constitute less than 1% of Greenland's area, contributed more than 12% of the net ice loss. This high-resolution record demonstrates that mass deficits extending over small spatial and temporal scales have made a relatively large contribution to recent ice sheet imbalance.**

## Index terms

## Keywords

## Introduction

Since the early 1990's, mass loss from the Greenland Ice Sheet has contributed approximately 10% of the observed global mean sea level rise [*Vaughan et al.*, 2013]. During this period, the ice imbalance has increased with time [*Rignot et al.*, 2011; *Shepherd et al.*, 2012], as warmer atmospheric conditions have prevailed [*Hanna et al.*, 2008; *Fettweis et al.*, 2013a, 2013b] and many marine terminating glaciers have accelerated [*Joughin et al.*, 2010; *Moon et al.*, 2012; *Enderlin et al.*, 2014]. Between 2000 and 2008 ice loss was due, in almost equal measures, to decreased surface mass balance (SMB) and increased ice discharge [*van den Broeke et al.*, 2009]. Since then, several exceptionally warm summers [*Hanna et al.*, 2012] have produced episodes of widespread surface melt [*Nghiem et al.*, 2012; *Fettweis et al.*, 2013b]. These conditions, which have been linked to the advection of warmer southerly air over the ice sheet [*Fettweis et al.*, 2013a; *Tedesco et al.*, 2013], have further increased annual ice losses from atmospheric melting, and subsequent runoff [*Schrama et al.*, 2014]. As a result, between 2009 and 2012 surface mass balance increased its contribution to 70% of the total ice sheet imbalance [*Enderlin et al.*, 2014].

Recent monitoring of the Greenland Ice Sheet has illustrated the high temporal and spatial variability in ice loss [*Rignot et al.*, 2011; *Moon et al.*, 2012; *Csatho et al.*, 2014; *Enderlin et al.*, 2014; *Schrama et al.*, 2014]. In 2012, annual mass losses of approximately 500 Gt were recorded [*Tedesco et al.*, 2013], representing the largest deficit of the observational era, yet these were followed in 2013 by a return to a state of near balance [*Khan et al.*, 2015]. Similarly, there has been substantial inter- and intra-regional variability in glacier dynamics [*Moon et al.*, 2012], as the response of individual systems to regional climatic forcing can be modulated by varying glacier geometry and setting. The high spatial and temporal variability in Greenland glacier behaviour complicates extrapolation of recent observations forward in time, and reinforces the need to develop process-based projections of ice sheet evolution. This requires an understanding of the drivers and timescales of ice sheet change, which in turn demands observations of ice sheet mass evolution sampled with sufficiently high spatial and temporal frequency to resolve this variability. Previous studies have demonstrated that CryoSat-2 radar altimetry can successfully resolve changes in ice sheet elevation and volume [*Helm et al.*, 2014].

Here, we use CryoSat-2 radar altimetry to produce high spatial (5 km) and temporal (monthly) records of Greenland Ice Sheet mass evolution, and use these measurements to resolve the detailed pattern of ice loss between 2011 and 2014.

## Data and Methods

We used CryoSat-2 radar altimetry to compute both linear rates of Greenland mass balance and monthly ice mass evolution between 1$^{st}$ January 2011 and 31$^{st}$ December 2014. We computed rates of elevation change within 5 x 5 km grid cells using a model fit method [*Smith et al.*, 2009; *Flament and Rémy*, 2012; *McMillan et al.*, 2014a] to partition the elevation fluctuations recorded within each grid cell, according to the contributions from topography, temporal changes in elevation and varying radar backscatter. The model was adapted from previous studies [*McMillan et al.*, 2014a, 2014b] to account for the impact of changing snowpack characteristics on the backscattered echo. Varying snowpack liquid water content, density and roughness can alter the depth distribution of the backscattered energy and impact upon radar altimeter elevation measurements [*Scott et al.*, 2006; *Gray et al.*, 2015]. Although we expect seasonal cycles in backscatter depth to have only a limited impact on longer-term elevation trends, more occasional, episodic changes in scattering characteristics have the potential to introduce larger artefacts into the elevation record. Such an effect occurred over the Greenland Ice Sheet interior during the summer of 2012 [*Nilsson et al.*, 2015] when approximately one third of the ice sheet experienced melt for the first time in a decade [*Tedesco et al.*, 2013].

To investigate the impact of the 2012 melt event on the radar altimeter measurements, we applied a numerical deconvolution procedure [*Arthern et al.*, 2001] to radar echoes acquired across the ice sheet interior during this time (see Auxiliary Material Section 2). This enabled us to estimate the distribution of backscattered power as a function of depth within the snowpack, by removing the contribution from reflections within the radar beam footprint that were beyond the point of closest approach. This analysis suggested that after the interior of the ice sheet experienced melt conditions in July 2012, there was a widespread transition from volume to surface scattering, a sharp increase in the extinction coefficient, and an abrupt increase in the elevation recorded by the altimeter (Auxiliary

Material Section 2), consistent with the interpretation of *Nilsson et al.* [2015]. We therefore adapted our model fit approach to accommodate this abrupt shift in dominant scattering horizon across the ice sheet interior during July 2012, using a step change function to model the recorded elevation change associated with this event (Auxiliary Material Section 3). To evaluate our approach, we compared our results to 8149 estimates of elevation change derived from co-located IceBridge airborne altimetry measurements, acquired between March 2009 and May 2014 (figure 1). The mean difference in the elevation change rates (CryoSat-2 - IceBridge) was reduced from 9 cm/yr to 3 cm/yr by accounting for the 2012 melt event, and the standard deviation of the resulting differences was 65 cm/yr.

We then converted the altimeter-derived rates of change to estimates of Greenland mass balance. For this conversion two approaches are well-established. Either a density model is used, which accounts for known dynamic and SMB processes [*Davis et al.*, 2005; *Thomas et al.*, 2006; *Wingham et al.*, 2006; *Shepherd and Wingham*, 2007; *Sørensen et al.*, 2011], or simulations of firn column thickness change are removed from the observed signal to estimate the underlying ice imbalance [*Li and Zwally*, 2011; *Zwally et al.*, 2011]. With the latter approach, the modelled firn mass changes are then added back to the ice mass changes, to estimate the total mass balance. In this study, we choose to use the former method because (1) it avoids errors in the observed and modelled elevation rates being interpreted as widespread dynamic imbalance across the interior of the ice sheet, and (2) it eliminates the need to correct for the 50% - 70% of the observed signal that is due to surface processes [*van den Broeke et al.*, 2009; *Enderlin et al.*, 2014] in order to estimate the residual changes due to dynamic imbalance. Further comparison of the two methods is provided in the Discussions and in Section 6 of the Auxiliary Material.

In common with other recent altimetry estimates of Greenland mass balance [*Sørensen et al.*, 2011], prior to the volume-to-mass conversion we applied a firn compaction correction. This step was designed to account for mass-conserving fluctuations in the rate of firn compaction, as any deviation of this rate away from steady state conditions will cause an elevation change that is not associated with a change in mass [*Zwally et al.*, 2005]. Specifically, we removed the component of the observed rate of elevation change that was due to firn compaction anomalies during our study period, using simulations of firn compaction from the Institute for Marine and Atmospheric Research Utrecht Firn Densification Model (IMAU-FDM v1.0) [*Ligtenberg et al.*, 2011; *Kuipers Munneke et al.*, 2015]. We emphasize that this procedure is designed to correct solely for mass-conserving processes, in order to isolate signals related to changing ice sheet mass, and so we only remove the simulated elevation change due to firn compaction anomalies. This step does not remove the total firn column elevation change, which also includes surface mass deposition and removal. IMAU-FDM simulates the temporal evolution of firn compaction, meltwater percolation and refreezing, and temperature in a vertical, 1-D column of firn and ice. The model is forced at its upper boundary by RACMO2.3, the most recent version of the RACMO regional climate model [*Noël et al.*, 2015]. Both models operate at 11 x 11 km spatial resolution.

To convert the resulting altimeter rates of change to mass, we constructed a density model that accounted for both surface and dynamic processes. In regions where high rates of elevation change and ice flow suggested a state of dynamic imbalance, we used an ice density of 917 kg m$^{-3}$ (see Auxiliary Material Section 8). Elsewhere, detected elevation changes were assumed to be driven by SMB processes, and we used an ice density within the ablation zone and the density of the IMAU-FDM firn layers gained or lost across the remaining areas. We then estimated the total ice sheet mass balance by summing the individual grid cell contributions, and filled the 11% of grid cells where no elevation rate was retrieved, using a model based on elevation, latitude and velocity change (see Auxiliary Material Section 4). The total mass balance uncertainty was computed by estimating spatially correlated and uncorrelated uncertainty in the measured surface elevation change, associated with changing snowpack characteristics and measurement imprecision respectively. These were

combined with the uncertainties arising from the unobserved areas, the density model, and the magnitude of the Glacial Isostatic Adjustment (GIA) and elastic bedrock uplift signals (see Auxiliary Material Section 9).

We also used the CryoSat-2 measurements to compute time-varying mass evolution at monthly intervals, by using our model fit solution to isolate the change, with time, of elevation anomalies within each grid cell. These anomalies were averaged over monthly intervals, corrected for the influence of firn compaction and converted to mass using monthly densities from the IMAU-FDM, supplemented with our dynamic imbalance mask. Monthly densities were used in order to account for seasonal variations in the density of surface mass change. At each monthly time step, we then used a bilinear interpolation to fill unobserved regions between satellite ground tracks, integrated spatially to produce an ice sheet mass anomaly and scaled our results in accordance with the proportion of the mass balance field sampled. The latter step was used to account for the bias introduced by preferentially sampling high latitude and inland regions (see Auxiliary Material Section 6).

To evaluate our estimates of ice sheet mass balance, we used independent observations from GRACE satellite gravimetry and modelling results from the RACMO2.3 regional climate model. Monthly GRACE solutions from the University of Texas Center for Space Research (CSR), with maximum spherical harmonic degree 96, were used to estimate ice mass changes following the regional integration approach [*Swenson and Wahr*, 2002; *Horwath and Dietrich*, 2009]. The integration kernel was tailored to minimize the combined effect of GRACE errors and leakage errors, and specifically the sensitivity to mass change in the Canadian Arctic, although some impact from these glaciers inevitably remains. The estimate necessarily includes mass changes of peripheral glaciers, because the limited spatial resolution of GRACE prevents their separation without external information. We corrected for gravity field changes due to GIA using modelling results by *A et al.* [2013], based on the ICE-5G glaciation history [*Peltier*, 2004]. We estimated the uncertainty on GRACE Greenland mass trends based upon simulations of the leakage error and an analysis of the GIA correction uncertainty by *Velicogna and Wahr* [2013].

RACMO2.3 simulations [*Noël et al.*, 2015] were used to estimate the rates of mass change driven by surface processes during our study period. The rate of mass change was estimated from a linear fit to the modelled cumulative surface mass balance anomalies, relative to the 1960-1979 average. The associated uncertainty accounted for both systematic and time-varying model uncertainties, together with the precision of the linear fit (see Auxiliary Material Section 10).

## Results and Discussion

### *Regional variability in ice loss*

Between 1st January 2011 and 31st December 2014 we estimate that the Greenland Ice Sheet lost mass at a rate of 269 ± 51 Gt/yr. The high spatial resolution and comprehensive coverage provided by CryoSat-2 provides a detailed map of ice sheet mass balance, showing widespread ice loss at lower elevations, particularly along the western margin, with the highest rates of change located across several distinct glacier systems (figure 1). We find that in recent years the south-western sector has been the dominant source of mass loss, contributing 41% of the total 4 year deficit. In contrast, the north-east contributed only 10% of all losses, with the remainder split between the south-east (25%) and north-west (24%) sectors. Our observations indicate that although regional mass imbalance has been most pronounced at lower latitudes, ice has also been lost from much of the north-east and north-west margins. These findings, which are supported by the RACMO2.3 simulations (figure 1), provide observational evidence that atmospheric conditions are affecting the far north of the ice sheet.

The pattern of regional mass balance resolved by CryoSat-2 is broadly similar to that derived from satellite gravimetry (figure 1). Using GRACE, we find a total ice sheet mass balance over the same period of -279 ± 22 Gt/yr, although it is important to note that the GRACE estimate also integrates the mass change of peripheral ice caps, which in recent years have contributed a further 30-40 Gt/yr of ice loss [*Bolch et al.*, 2013]. In comparison to GRACE, the uncertainty associated with our CryoSat-2 estimate is relatively large, although the finer spatial detail is able to resolve mass balance at the scale of individual glacier catchments. The higher CryoSat-2 uncertainty largely reflects the difficulty in assessing the influence of spatially-correlated changes in snowpack properties. In this study, we have

estimated this uncertainty based upon the impact of the extreme 2012 melt event (Auxiliary Material Section 9), which yields an uncertainty slightly above the 45 Gt/yr that would be expected given the mean difference between the rates of elevation change recorded by CryoSat-2 and IceBridge altimetry. Further work is needed to formally constrain this component of the uncertainty budget.

Over the same spatial and temporal domain as our CryoSat-2 observations, RACMO2.3 indicates that atmospheric processes produced an annual SMB deficit of -154 ± 65 Gt/yr, which is equivalent to 57 % of the observed ice sheet mass balance. The difference of -115 ± 83 Gt/yr, which represents the mass loss due to other factors, is close to an independent estimate of 2009-2012 dynamic loss of 122 Gt/yr [*Enderlin et al.*, 2014], although our associated uncertainty is large when integrated over the whole ice sheet, reflecting the challenges of partitioning the observed signals across the entire ice sheet interior. We investigate the differences between the two datasets, and their utility for detecting dynamic imbalance at the more localised scale of individual glaciers catchments, in more detail below.

### *Temporal variability in ice loss*

Our monthly estimates of ice sheet mass evolution resolve the temporal variability associated with seasonal and inter-annual forcing, and also enable an assessment of the consistency between the CryoSat-2 and GRACE records (figure 2). Both techniques resolve large variations in annual ice loss. The CryoSat-2 measurements show that losses during the exceptionally warm summer of 2012 produced an annual ice deficit of 439 ± 62 Gt, which dominated the total four year period. In contrast, 2013 saw only moderate losses of 116 ± 65 Gt, which were approximately half the 2000-2011 mean [*Shepherd et al.*, 2012]. Comparing the monthly CryoSat-2 and GRACE estimates, we find close agreement (Pearson correlation coefficient, R, of 0.96) between the two independent approaches, albeit over their different spatial domains. This statistic reflects, in part, the consistency with which both methods resolve the long-term trend in mass loss. There is, however, also relatively good agreement (R = 0.78) in the seasonal and inter-annual variability, once the long-term trend is removed. The GRACE observations do tend to exhibit slightly larger amplitude seasonal cycles, and the 2012 deficit recorded by CryoSat-2 is lower than a previous GRACE estimate [*Tedesco et al.*,

2013]. This may be because of the incomplete sampling by CryoSat-2 of the full mass field at each monthly epoch, possible dampening effects caused by the CryoSat-2 backscatter correction, the limited sensitivity of radar altimetry to seasonal cycles in dry snow accumulation or the integration by GRACE of signals arising from peripheral ice caps and unglaciated regions.

Our record shows that during the survey period, annual ice losses varied by several hundred gigatonnes. Analysing the RACMO2.3 surface mass fluxes and comparing these with estimates of ice discharge from *Enderlin et al.* [2014] indicates that the dominant source of this variability was fluctuations in meltwater runoff. Whereas year-to-year differences in regionally-integrated solid ice discharge typically do not exceed 20 Gt/yr (~ 5 % of the mean) and inter-annual variability in snowfall is also relatively modest (1991-2014 standard deviation of 61 Gt/yr, or 9 % of the mean), meltwater runoff has exhibited much larger variability. Between 1991 and 2014, the standard deviation of annual runoff was 102 Gt/yr, or 28 % of the mean. In recent years, contrasting atmospheric conditions have driven even greater variability, with annual runoff of 625 Gt/yr and 298 Gt/yr in 2012 and 2013, respectively. In 2012, intense summer melting was driven by persistent high pressure, associated with a strong negative phase of the North Atlantic Oscillation (NAO) and a high Greenland Blocking Index [*Hanna et al.*, 2014]. In contrast, 2013 saw low-pressure and low-temperature conditions, coinciding with the most positive summertime NAO recorded in the past 20 years. Our record demonstrates the impact that these changing atmospheric conditions have had upon year-to-year variability in mass loss, and more specifically the potential for intense melt events lasting only a few months to make large contributions to multi-year mass balance.

### *Mass loss due to dynamic processes*

Differencing the CryoSat-2 and RACMO2.3 mass balance fields removed the simulated component due to atmospheric processes. This allowed us to investigate the discrepancies between the two datasets, due to model or observational errors, and to identify individual glacier systems where additional mass changes suggested dynamic imbalance (figure 3). To evaluate these signals, we also computed recent changes in glacier flow using repeated ice velocity measurements from 2000-2001 and 2008-2009 [*Joughin et al.*, 2010]. The CryoSat-2 and RAMCO2.3 datasets provide evidence of significant dynamic mass loss at five marine-terminating glaciers; Kangerdlugssuaq Glacier in the south-east; Jacobshavn, Upernavik Isstrøm, Steenstrup Glaciers on the western margin, and Zachariae Isstrøm in the north-east (figure 3a). Significant signals of dynamic imbalance are not apparent in the far south-east, which may relate to the incomplete sampling of these coastal regions. Comparing our mass loss and velocity measurements, we find that each of the five glaciers identified above has undergone a significant increase in velocity during the preceding decade (figure 3b), suggesting that deficits in mass associated with these flow accelerations have continued throughout the duration of this study. With its interferometric capability, CryoSat-2 is able to sample 67 % of the near-terminus areas of these glaciers where the dynamic imbalance is most pronounced. These regions, which together constitute only 0.9 % of the total ice sheet area, have contributed more than 12 % of the total mass balance during our study period. In contrast, Storstrømmen in the north-east is the only glacier where we detect dynamically-driven mass gain. This is likely to be an ongoing response to flow deceleration since the glacier surged between 1978 and 1984 [*Mohr et al.*, 1998].

Our results demonstrate the capability of interferometric altimetry and regional climate modelling to monitor ice dynamic imbalance at the catchment scale. At the highest elevations, however, CryoSat-2 tends to show more negative mass change than RACMO2.3, whereas across some land-terminating sectors, particularly in the south-west, the reverse is found. Although multi-decadal deceleration in ice velocity has been observed across parts of the ablation zone of western Greenland [*van de Wal et al.*, 2008; *Tedstone et al.*, 2015], direct evidence of changes in strain rate and associated dynamic thickening, is still lacking. Rather, we believe that these observed differences within the interior are

indicative of the respective uncertainties associated with the two datasets. These may arise from uncompensated altimeter signals related to changing snowpack characteristics, the initialization profile used by the firn densification model, or the inability of RACMO2.3 to completely reproduce the temporal variability in the cumulative surface mass balance anomaly. Together, these differences reflect the current challenges associated with mapping and modelling Greenland mass balance fields at high resolution and motivate our decision to employ a density model based approach within this study (Auxiliary Material Section 6). Nonetheless, other altimeter-based methods have been advocated within the community, whereby the difference between the total (observed) and SMB (modelled) components of mass change are used to estimate the underlying ice imbalance across the entire ice sheet. For comparison we therefore also compute mass change using this approach. This method yields an estimated mass balance of -230 Gt/yr, which is 39 Gt/yr more positive than our chosen approach, because it attributes all residual signals across slow flowing regions to result from dynamic imbalance. Determining with confidence the extent of any dynamic changes across the slow flowing interior remains, we believe, a challenge and a principle avenue for future research.

## Conclusions

Using CryoSat-2 radar altimetry, and the RACMO2.3 and IMAU-FDM models, we have computed Greenland Ice Sheet mass balance at high spatial and temporal resolution. Despite the challenges associated with radar wave interaction with a highly variable snowpack, we find a good level of agreement with both airborne altimetry and satellite gravimetry. Between January 2011 and December 2014 we estimate that the Greenland Ice Sheet lost an average of 269 ± 51 Gt/yr of snow and ice. The observed deficit indicates an annual contribution of 0.74 ± 0.14 mm/yr to global mean sea level, which is approximately double the 1992-2011 mean [*Shepherd et al.*, 2012]. Since 2011, ice sheet mass balance has been highly variable in space and time. After the record deficit of 439 ± 62 Gt observed in 2012, which was driven by an exceptionally warm summer, subsequent ice losses have been more moderate. Combining altimetry and regional atmospheric model simulations, we identify five glacier systems which currently exhibit negative ice dynamic balance, all of which have

undergone significant changes in velocity during the preceding decade. Our results suggest that future Synthetic Aperture Radar altimetry missions can contribute towards monitoring and understanding ongoing Greenland mass balance at the scale of individual glacier systems.

## Acknowledgements

## References

A, G., J. Wahr, and S. Zhong (2013), Computations of the viscoelastic response of a 3-D compressible earth to surface loading: An application to glacial isostatic adjustment in Antarctica and Canada, *Geophys. J. Int.*, *192*(2), 557–572, doi:10.1093/gji/ggs030.

van Angelen, J. H., M. R. van den Broeke, B. Wouters, and J. T. M. Lenaerts (2013), Contemporary (1960-2012) Evolution of the Climate and Surface Mass Balance of the Greenland Ice Sheet, *Surv. Geophys.*, *35*, 1155–1174, doi:10.1007/s10712-013-9261-z.

Arthern, R. J., D. J. Wingham, and A. L. Ridout (2001), Controls on ERS altimeter measurements over ice sheets: Footprint-scale topography, backscatter fluctuations, and the dependence of microwave penetration depth on saetllite orientation, *J. Geophys. Res.*, *106*(D24), 33,471–33,484.

Bolch, T., L. Sandberg Sørensen, S. B. Simonsen, N. Mölg, H. MacHguth, P. Rastner, and F. Paul (2013), Mass loss of Greenland's glaciers and ice caps 2003-2008 revealed from ICESat laser

altimetry data, *Geophys. Res. Lett.*, *40*(5), 875–881, doi:10.1002/grl.50270.

van den Broeke, M., J. Bamber, J. Ettema, E. Rignot, E. Schrama, W. J. van de Berg, E. van Meijgaard, I. Velicogna, and B. Wouters (2009), Partitioning recent Greenland mass loss., *Science (80-. ).*, *326*(5955), 984–6, doi:10.1126/science.1178176.

Csatho, B. M., A. F. Schenk, C. J. van der Veen, G. Babonis, K. Duncan, S. Rezvanbehbahani, M. R. van den Broeke, S. B. Simonsen, S. Nagarajan, and J. H. van Angelen (2014), Laser altimetry reveals complex pattern of Greenland Ice Sheet dynamics., *Proc. Natl. Acad. Sci. U. S. A.*, *111*(52), 18478–83, doi:10.1073/pnas.1411680112.

Davis, C., and A. Ferguson (2004a), Elevation change of the Antarctic ice sheet, 1995-2000, from ERS-2 satellite radar altimetry, *IEEE Trans. Geosci. Remote Sens.*, *42*(11), 2437–2445, doi:10.1109/TGRS.2004.836789.

Davis, C. H., and A. C. Ferguson (2004b), Elevation Change of the Antarctic Ice Sheet , Radar Altimetry, *IEEE Trans. Geosci. Remote Sens.*, *42*(11), 1995–2000.Davis, C. H., Y. H. Li, J. R. McConnell, M. M. Frey, and E. Hanna (2005), Snowfall-driven growth in East Antarctic ice sheet mitigates recent sea-level rise, *Science (80-. ).*, *308*(5730), 1898–1901, doi:10.1126/science.1110662.

Davis, C. H., Y. H. Li, J. R. McConnell, M. M. Frey, and E. Hanna (2005), Snowfall-driven growth in East Antarctic ice sheet mitigates recent sea-level rise, *Science (80-. ).*, *308*(5730), 1898–1901, doi:10.1126/science.1110662.

Enderlin, E., I. Howat, S. Jeong, M. Noh, J. van Angelen, and M. van den Broeke (2014), An improved mass budget for the Greenland ice sheet, *Geophys. Res. Lett.*, *41*, 1–7, doi:10.1002/2013GL059010.

Ettema, J., M. R. van den Broeke, E. van Meijgaard, W. J. van de Berg, J. L. Bamber, J. E. Box, and R. C. Bales (2009), Higher surface mass balance of the Greenland ice sheet revealed by high-resolution climate modeling, *Geophys. Res. Lett.*, *36*(12), L12501, doi:10.1029/2009GL038110.

Fettweis, X., E. Hanna, C. Lang, A. Belleflamme, M. Erpicum, and H. Gall (2013a), Brief communication "Important role of the mid-tropospheric atmospheric circulation in the recent surface melt increase over the Greenland ice sheet," *Cryosph.*, *7*, 241–248, doi:10.5194/tc-7-241-2013.

Fettweis, X., B. Franco, M. Tedesco, J. H. Van Angelen, J. T. M. Lenaerts, M. R. Van Den Broeke, and H. Gallee (2013b), Estimating the Greenland ice sheet surface mass balance contribution to future sea level rise using the regional atmospheric climate model MAR, *Cryosph.*, *7*, 469–489, doi:10.5194/tc-7-469-2013.

Flament, T., and F. Rémy (2012), Dynamic thinning of Antarctic glaciers from along-track repeat radar altimetry, *J. Glaciol.*, *58*(211), 830–840, doi:10.3189/2012JoG11J118.

Gray, L., D. Burgess, L. Copland, M. N. Demuth, T. Dunse, K. Langley, and T. V. Schuler (2015), CryoSat-2 delivers monthly and inter-annual surface elevation change for Arctic ice caps, *Cryosph. Discuss.*, *9*(3), 2821–2865, doi:10.5194/tcd-9-2821-2015.

Hanna, E., P. Huybrechts, K. Steffen, J. Cappelen, R. Huff, C. Shuman, T. Irvine-Fynn, S. Wise, and M. Griffiths (2008), Increased runoff from melt from the Greenland Ice Sheet: A response to

global warming, *J. Clim.*, *21*(2), 331–341, doi:10.1175/2007JCLI1964.1.

Hanna, E., S. H. Mernild, J. Cappelen, and K. Steffen (2012), Recent warming in Greenland in a climatic context: I. Evaluation of surface air temperature records, *Environ. Res. Lett.*, *7*, doi:10.1088/1748-9326/7/4/045404.

Hanna, E., X. Fettweis, S. H. Mernild, J. Cappelen, M. H. Ribergaard, C. A. Shuman, K. Steffen, L. Wood, and T. L. Mote (2014), Atmospheric and oceanic climate forcing of the exceptional Greenland ice sheet surface melt in summer 2012, *Int. J. Climatol.*, *34*(4), 1022–1037, doi:10.1002/joc.3743.

Haran, T., J. Bohlander, T. Scambos, T. Painter, and M. Fahnestock (2013), MODIS Mosaic of Greenland (MOG) Image Map, Version 1, *Boulder, Color. USA. NSIDC Natl. Snow Ice Data Cent.*

Helm, V., a. Humbert, and H. Miller (2014), Elevation and elevation change of Greenland and Antarctica derived from CryoSat-2, *Cryosph.*, *8*(4), 1539–1559, doi:10.5194/tc-8-1539-2014.

Horwath, M., and R. Dietrich (2009), Signal and error in mass change inferences from GRACE: the case of Antarctica, *Geophys. J. Int.*, *177*, 849–864, doi:10.1111/j.1365-246X.2009.04139.x.

Joughin, I., B. E. Smith, I. M. Howat, T. Scambos, and T. Moon (2010), Greenland flow variability from ice-sheet-wide velocity mapping, *J. Glaciol.*, *56*(197), 415–430.

Krabill, W. (2014), IceBridge ATM L2 Icessn Elevation, Slope, and Roughness. Version 2, *NASA DAAC Natl. Snow Ice Data Center., Boulder, CO, USA*.

Khan, S. A., A. Aschwanden, A. a. Bjørk, J. Wahr, K. K. Kjeldsen, and K. H. Kjaer (2015), Greenland ice sheet mass balance: a review, *Reports Prog. Phys.*, *046801*, 1–26, doi:10.1088/0034-4885/78/4/046801.

Kuipers Munneke, P. et al. (2015), Elevation change of the Greenland ice sheet due to surface mass balance and firn processes, 1960–2013, *Cryosph. Discuss.*, *9*(3), 3541–3580, doi:10.5194/tcd-9-3541-2015.

Li, J., and H. J. Zwally (2011), Modeling of firn compaction for estimating ice-sheet mass change from observed ice-sheet elevation change, *Ann. Glaciol.*, *52*(59), 1–7, doi:10.3189/172756411799096321.

Ligtenberg, S. R. M., M. M. Helsen, and M. R. Van Den Broeke (2011), An improved semi-empirical model for the densification of Antarctic firn, *Cryosphere*, *5*(4), 809–819, doi:10.5194/tc-5-809-2011.

McMillan, M., A. Shepherd, A. Sundal, K. Briggs, A. Muir, A. Ridout, A. Hogg, and D. Wingham (2014a), Increased ice losses from Antarctica detected by CryoSat-2, *Geophys. Res. Lett.*, *41*, 1–7, doi:10.1002/2014GL060111.

McMillan, M. et al. (2014b), Rapid dynamic activation of a marine-based Arctic ice cap, *Geophys. Res. Lett.*, *41*, 8902–8909, doi:10.1002/2014GL062255.

Mohr, J. J., N. Reeh, and S. N. Madsen (1998), Three-dimensional glacial flow and surface elevation measured with radar interferometry, *Nature*, *391*(6664), 273–276, doi:10.1038/34635.

Moon, T., I. Joughin, B. E. Smith, and I. M. Howat (2012), 21st-Century Evolution of Greenland

Outlet Glacier Velocities, *Science (80-. ).*, *336*(576), doi:10.1126/science.1219985.

Nghiem, S. V, D. K. Hall, T. L. Mote, M. Tedesco, M. R. Albert, K. Keegan, C. A. Shuman, N. E. DiGirolamo, and G. Neumann (2012), The extreme melt across the Greenland ice sheet in 2012, *Geophys. Res. Lett.*, *39*, L20502, doi:10.1029/2012GL053611.

Nilsson, J. et al. (2015), Greenland 2012 melt event effects on CryoSat-2 radar altimetry, *Geophys. Res. Lett.*, *42*(10), 3919–3926, doi:10.1002/2015GL063296.

Noël, B., W. J. van de Berg, E. van Meijgaard, P. Kuipers Munneke, R. S. W. van de Wal, and M. R. van den Broeke (2015), Evaluation of the updated regional climate model RACMO2.3: summer snowfall impact on the Greenland Ice Sheet, *Cryosph.*, *9*(5), 1831–1844, doi:10.5194/tc-9-1831-2015.

Peltier, W. R. (2004), Global Glacial Isostasy and the Surface of the Ice-Age Earth: The ICE-5G (VM2) Model and GRACE, *Annu. Rev. Earth Planet. Sci.*, *32*(1), 111–149, doi:10.1146/annurev.earth.32.082503.144359.

Rignot, E., I. Velicogna, M. R. van den Broeke, A. Monaghan, and J. Lenaerts (2011), Acceleration of the contribution of the Greenland and Antarctic ice sheets to sea level rise, *Geophys. Res. Lett.*, *38*, doi:10.1029/2011GL046583.

Schrama, E. J. O., B. Wouters, and R. Rietbroek (2014), A mascon approach to assess ice sheet and glacier mass balances and their uncertainties from GRACE data, *J. Geophys. Res.*, (February 2003), doi:10.1002/2013JB010923.

Scott, J. B. T., P. Nienow, D. Mair, V. Parry, E. Morris, and D. J. Wingham (2006), Importance of seasonal and annual layers in controlling backscatter to radar altimeters across the percolation zone of an ice sheet, *Geophys. Res. Lett.*, *33*(24), L24502, doi:10.1029/2006GL027974.

Shepherd, A., and D. Wingham (2007), Recent sea-level contributions of the Antarctic and Greenland ice sheets, *Science (80-. ).*, *315*(5818), 1529–1532.

Shepherd, A. et al. (2012), A reconciled estimate of ice-sheet mass balance., *Science (80-. ).*, *338*(6111), 1183–9, doi:10.1126/science.1228102.

Smith, B., H. A. Fricker, I. Joughin, and S. Tulaczyk (2009), An inventory of active subglacial lakes in Antarctica detected by ICESat (2003-2008), *J. Glaciol.*, *55*(192), 573–595.

Sørensen, L. S., S. B. Simonsen, K. Nielsen, P. Lucas-Picher, G. Spada, G. Adalgeirsdottir, R. Forsberg, and C. S. Hvidberg (2011), Mass balance of the Greenland ice sheet (2003–2008) from ICESat data – the impact of interpolation, sampling and firn density, *Cryosph.*, *5*, 173–186, doi:10.5194/tc-5-173-2011.

Swenson, S., and J. Wahr (2002), Methods for inferring regional surface-mass anomalies from Gravity Recovery and Climate Experiment (GRACE) measurements of time-variable gravity, *J. Geophys. Res.*, *107*(B9), 2193, doi:10.1029/2001JB000576.

Tedesco, M., X. Fettweis, T. Mote, J. Wahr, P. Alexander, J. E. Box, and B. Wouters (2013), Evidence and analysis of 2012 Greenland records from spaceborne observations, a regional climate model and reanalysis data, *Cryosph.*, *7*(2), 615–630, doi:10.5194/tc-7-615-2013.

Tedstone, A. J., P. W. Nienow, N. Gourmelen, A. Dehecq, D. Goldberg, and E. Hanna (2015),

Decadal slowdown of a land-terminating sector of the Greenland Ice Sheet despite warming, *Nature*, *526*(7575), 692–695, doi:10.1038/nature15722.

Thomas, R., E. Frederick, W. Krabill, S. Manizade, and C. Martin (2006), Progressive increase in ice loss from Greenland, *Geophys. Res. Lett.*, *33*(10), n/a–n/a, doi:10.1029/2006GL026075.

Unden, P. et al. (2002), HIRLAM-5 Scientific Documentation, *HIRLAM-5 Proj.*

Vaughan, D. G. et al. (2013), Observations: Cryosphere., in *Climate Change 2013: Physical Science Basis. Contribution of Working Group I to the Fifth Assessment Report of the Intergovernmental Panel on Climate Change*, edited by V. B. and P. M. M. (eds. . Stocker, T.F., D. Qin, G.-K. Plattner, M. Tignor, S.K. Allen, J. Boschung, A. Nauels, Y. Xia, Cambridge University Press, Cambridge, UK.

Velicogna, I., and J. Wahr (2013), Time-variable gravity observations of ice sheet mass balance: Precision and limitations of the GRACE satellite data, *Geophys. Res. Lett.*, *40*(12), 3055–3063, doi:10.1002/grl.50527.

van de Wal, R. S. W., W. Boot, M. R. van den Broeke, C. J. P. P. Smeets, C. H. Reijmer, J. J. a. Donker, and J. Oerlemans (2008), Large and Rapid Melt-Induced Velocity Changes in the Ablation Zone of the Greenland Ice Sheet, *Science (80-. ).*, *321*(5885), 111–113, doi:10.1126/science.1158540.

Wingham, D. J., L. Phalippou, C. Mavrocordatos, and D. Wallis (2004), The mean echo and echo cross product from a beamforming interferometric altimeter and their application to elevation measurement, *IEEE Trans. Geosci. Remote Sens.*, *42*(10), 2305–2323, doi:10.1109/TGRS.2004.834352.

Wingham, D. J., A. Shepherd, A. Muir, and G. J. Marshall (2006), Mass balance of the Antarctic ice sheet, *Philos. Trans. R. Soc. A-MATHEMATICAL Phys. Eng. Sci.*, *364*(1844), 1627–1635, doi:10.1098/rsta.2006.1792.

Zwally, H. J., M. B. Giovinetto, J. Li, H. G. Cornejo, M. A. Beckley, A. C. Brenner, J. L. Saba, and D. Yi (2005), Mass changes of the Greenland and Antarctic ice sheets and shelves and contributions to sea-level rise : 1992 – 2002, *J. Glaciol.*, *51*(175), 1992–2002.

Zwally, H. J. et al. (2011), Greenland ice sheet mass balance: distribution of increased mass loss with climate warming; 2003–07 versus 1992–2002, *J. Glaciol.*, *57*(201), 88–102, doi:10.3189/002214311795306682.
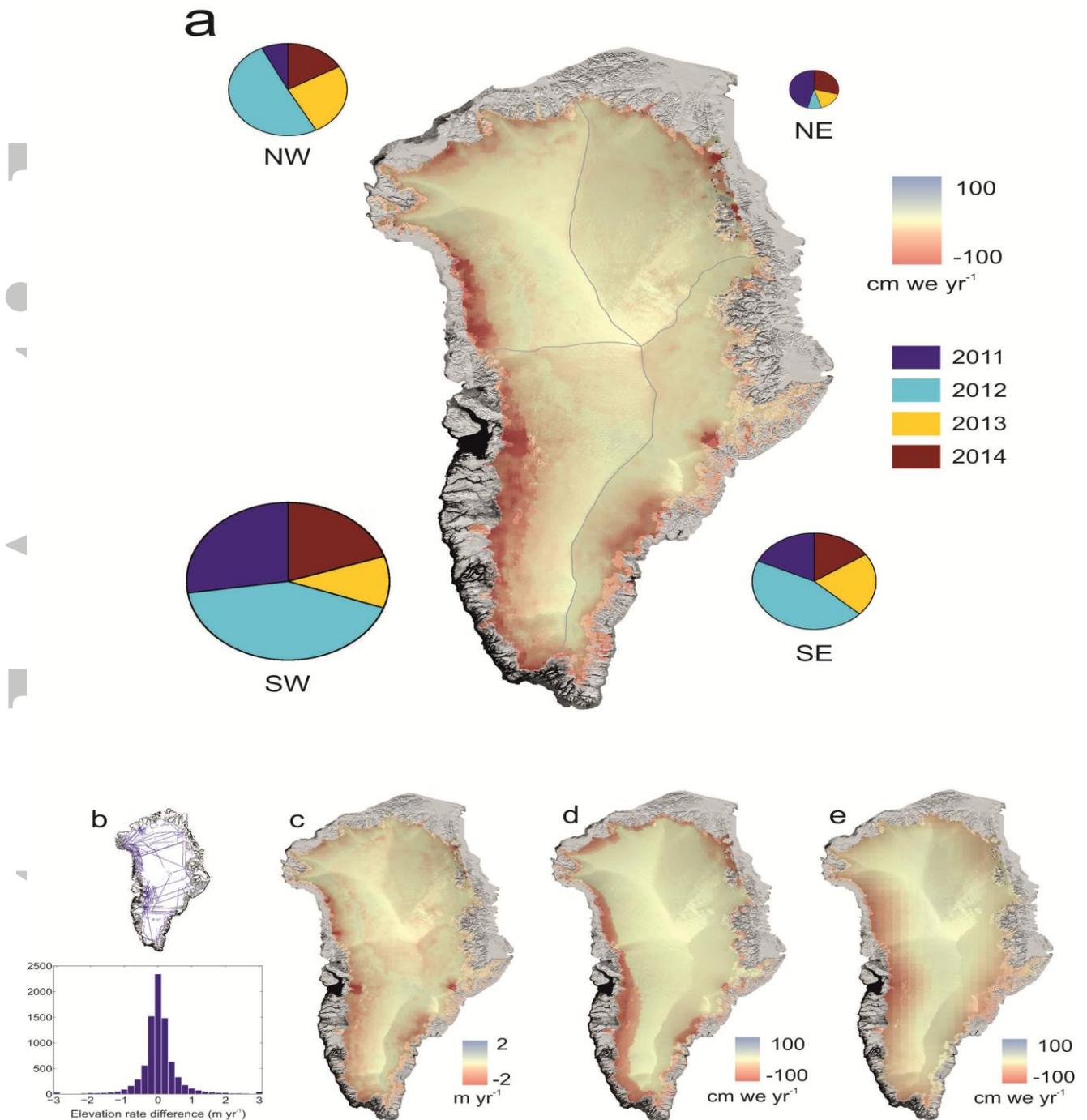
**Figure 1. Greenland mass and elevation change.** a. Rate of mass change between January 2011 and December 2014 from CryoSat-2 radar altimetry and firn modelling. For each of the southwest (SW), southeast (SE), northeast (NE) and northwest (NW) sectors, the color wheel indicates the proportion of mass lost in each year, with the radius scaled according to the magnitude of the total losses. The boundaries between the four sectors are shown in gray. b. The distribution of IceBridge airborne altimetry tracks used for validation and a histogram of the differences (CryoSat-2 minus IceBridge) in the recorded rates of elevation change. c. Rate of elevation change between 2011 and 2014 from

CryoSat-2 radar altimetry. d. Simulated 2011-2014 rate of mass change due to surface processes from RACMO2.3 regional climate modelling. e. Rate of mass change between 2011 and 2014 from GRACE gravimetry. The background image is the MODIS mosaic of Greenland [*Haran et al.*, 2013] overlaid with a shaded relief of ice sheet elevation.
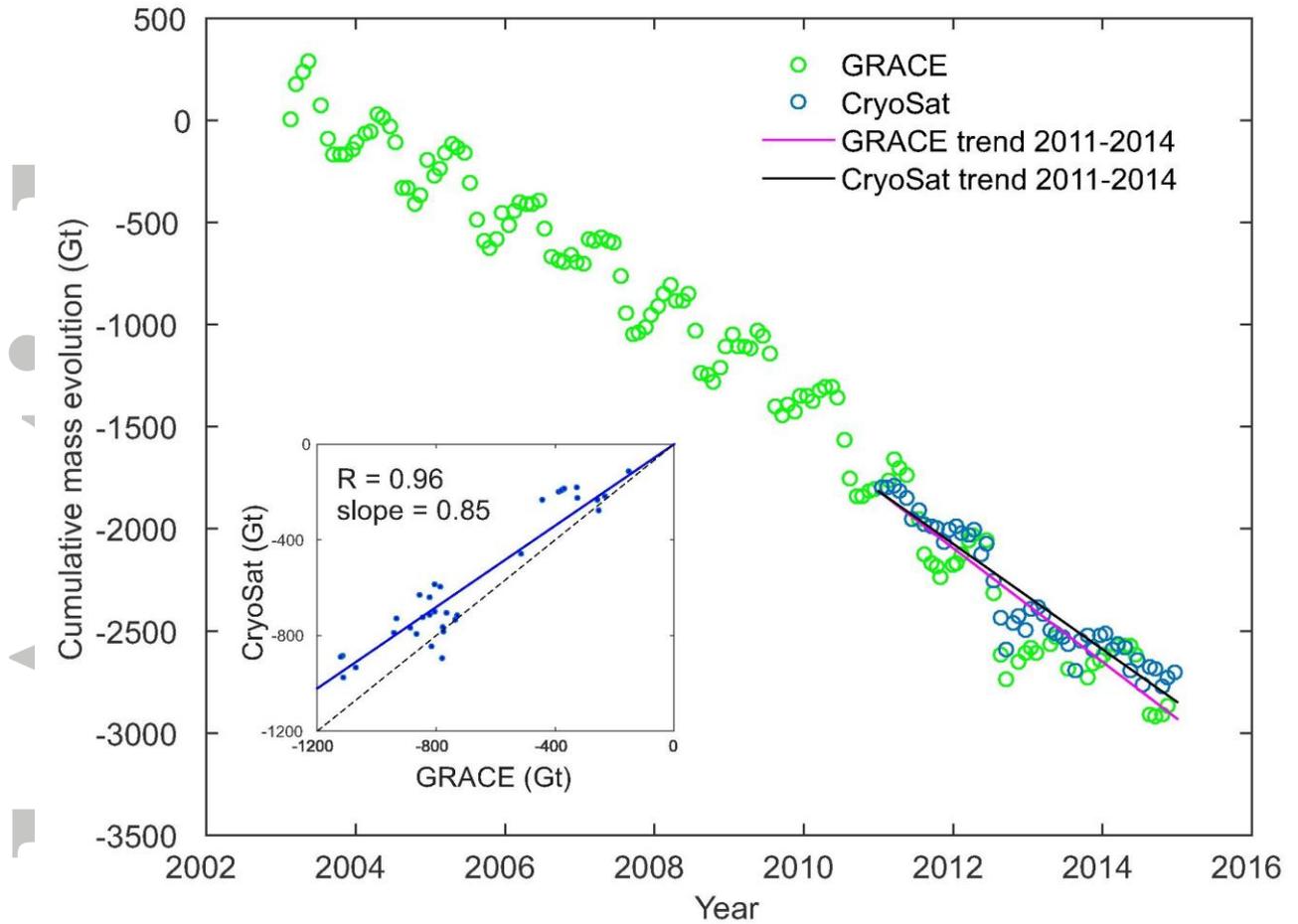
**Figure 2. Greenland mass evolution.** Monthly evolution in ice sheet mass since 2003 from GRACE gravimetry (green) and since 2011 from CryoSat-2 altimetry and firn modelling (blue). The CryoSat-2 time-series has been referenced to the GRACE data at the start of 2011. The inset shows the correspondence between the GRACE and CryoSat-2 monthly estimates of mass evolution since 2011 (solid blue dots), together with a linear regression (solid blue line), the regression slope and the Pearson correlation coefficient, R. The dashed line indicates equivalence, although the GRACE results include, additionally, mass changes of peripheral ice caps and unglaciated regions.
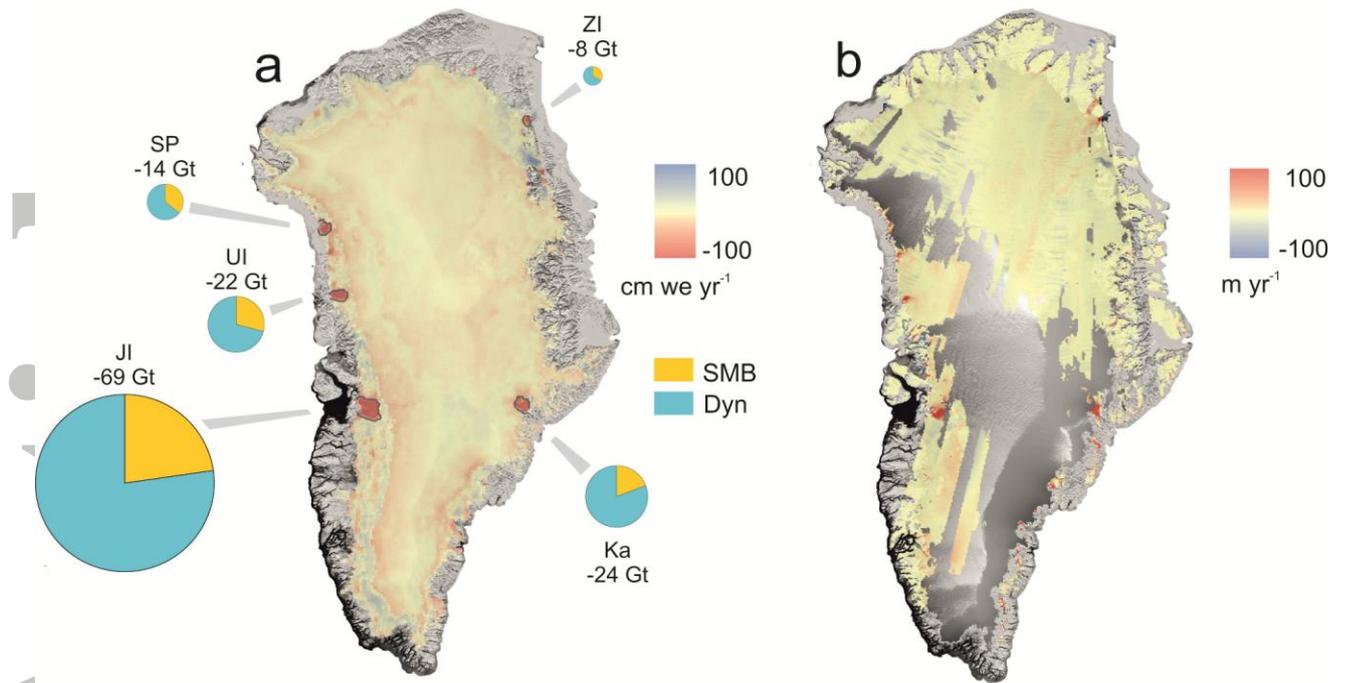
**Figure 3. Greenland dynamic mass balance, 2011-2014.** a. Difference between Cryosat-2 and RACMO2.3 mass balance. b. Ice velocity change between 2000-2001 and 2008-2009 mapped by imaging Synthetic Aperture Radar [*Joughin et al.*, 2010]. Several marine-terminating glaciers exhibiting signs of dynamic ice loss are apparent; Kangerdlugssuaq (Ka) Jacobshavn Isbræ (JI), Upernavik Isstrøm (UI), Steenstrup (SP) and Zachariae Isstrøm (ZI); all of which have undergone velocity change during the preceding decade. For each of these glaciers, the total 4-year mass loss from the rapidly thinning terminus regions, bounded by the gray lines, is shown. The color wheels indicate the partitioning of mass losses within the bounded regions, according to surface mass and dynamic processes, with the radius of each wheel scaled according to the magnitude of the total losses. The background image is the MODIS mosaic of Greenland [*Haran et al.*, 2013] overlaid with a shaded relief of ice sheet elevation.